Author Manuscript

Author Manuscript

Author Manuscript

Author Manuscript

HHS Public Access

Author manuscript

Nat Med. Author manuscript; available in PMC 2013 November 01.

Published in final edited form as:

Nat Med. 2013 May ; 19(5): 646–651. doi:10.1038/nm.3154.

Regeneration and Experimental Orthotopic Transplantation of a Bioengineered Kidney

Jeremy J Song, BS[2,4], **Jacques Guyette, PhD**[2,4], **Sarah Gilpin, PhD**[2,4], **Gabriel Gonzalez, PhD**[2,4], **Joseph P Vacanti, MD**[2,3,4], and **Harald C Ott, MD, PD**[1,2,4]

[1]Division of Thoracic Surgery, Department of Surgery, Massachusetts General Hospital

[2]Center for Regenerative Medicine, Massachusetts General Hospital

[3]Division of Pediatric Surgery, Department of Surgery, Massachusetts General Hospital

[4]Harvard Medical School

Abstract

Over 100,000 individuals in the United States currently await kidney transplantation, while 400,000 individuals live with end-stage kidney disease requiring hemodialysis. The creation of a transplantable graft to permanently replace kidney function would address donor organ shortage and the morbidity associated with immunosuppression. Such a bioengineered graft must have the kidney's architecture and function, and permit perfusion, filtration, secretion, absorption, and drainage of urine. We decellularized rat, porcine, and human kidneys by detergent perfusion, yielding acellular scaffolds with vascular, cortical and medullary architecture, collecting system and ureters. To regenerate functional tissue, we seeded rat kidney scaffolds with epithelial and endothelial cells, then perfused these cell-seeded constructs in a whole organ bioreactor. The resulting grafts produced rudimentary urine *in vitro* when perfused via their intrinsic vascular bed. When transplanted in orthotopic position in rat, the grafts were perfused by the recipient's circulation, and produced urine via the ureteral conduit *in vivo*.

Nearly one million patients in the US live with end stage renal disease (ESRD) with over 100,000 new diagnoses every year[1]. Although hemodialysis has increased survivorship of those with end-stage renal disease (ESRD), transplantation remains the only available curative treatment. About 18,000 kidney transplants are performed per year in the United

Users may view, print, copy, download and text and data- mine the content in such documents, for the purposes of academic research, subject always to the full Conditions of use: http://www.nature.com/authors/editorial_policies/license.html#terms

Corresponding Author: Harald C Ott, MD, PD, Harvard Medical School, Division of Thoracic Surgery, Department of Surgery, Massachusetts General Hospital, 55 Fruit Street, GRB – 425, Boston, MA 02114, hott@partners.org.

Author contributions

H.C.O. conceived, designed and oversaw all of the studies, collection of results, interpretation of the data, and writing of the manuscript. He was responsible for the primary undertaking, completion and supervision of all experiments. J.S. and J.G. performed animal surgeries, conducted decellularization, and whole organ culture experiments, and performed *in vitro* and *in vivo* testing. S.G. was responsible for cell culture, preparation of cell suspensions, and matrix characterization. G.G. characterized fetal lung cells, scaffolds, and regenerated constructs using various imaging techniques. J.P.V. provided input on tissue engineering aspects and reviewed the manuscript.

Competing financial interest

The authors declare no competing financial interests.

Author Manuscript Author Manuscript Author Manuscript Author Manuscript

States[1], yet approximately 100,000 Americans currently await a donor kidney[2]. Stagnant donor organ numbers increase waiting times over three years and waitlist mortality to 5-10%. Despite advances in renal transplant immunology[3], 20% of recipients will experience an episode of acute rejection within five years of transplantation, and approximately 40% of recipients will die or loose graft function within ten years after transplantation. Creation of a bioengineered kidney could theoretically bypass these problems by providing an autologous graft on demand.

Hemofiltration and hemodialysis use an acellular semipermeable membrane to substitute the native kidney's functions. Several attempts have been made to bioengineer viable tubular structures to further supplement hemofiltration with cell dependent functions[4,5]. When hemofiltration devices were combined with bioengineered renal tubules, the resulting bioartificial kidney (BAK) replaced renal function in uremic dogs[6] and temporarily improved renal function in patients with acute renal failure[7,8]. In an alternative approach, kidney primordia have been shown to develop into a functional organ *in vivo* and prolong life when transplanted into anephric rats[9]. Devices to make renal assist devices more portable[10] or even implantable[11] have reached the stage of preclinical evaluation and hold tremendous promise to improve the quality of life of patients in end stage renal failure. A key step towards a fully implantable, permanent graft is the development of a biocompatible scaffold that facilitates cell engraftment and function, and allows full recipient integration via blood perfusion.

Based on our prior experience with whole organ heart[12] and lung[13] extracellular matrix (ECM) scaffolds, we hypothesized that the native kidney ECM could provide such a scaffold for subsequent cell seeding. In prior studies, detergents removed cells from native kidney ECM while preserving biomechanical properties and matrix protein characteristics in tissue slices[14] and whole organs[15-18]. We therefore decellularized kidneys via detergent perfusion to create whole organ scaffolds with intact and perfusable vascular, glomerular, and tubular compartments. We then repopulated decellularized kidney scaffolds with endothelial and epithelial cells. *In vitro* biomimetic culture via arterial perfusion led to the formation of functional renal grafts. To test *in vivo* host integration and function, we transplanted bioengineered kidneys in orthotopic position and documented urine production.

Results

Perfusion decellularization of cadaveric kidneys

Cadaveric rat kidneys were decellularized via renal artery perfusion with 1% sodium dodecyl sulfate (SDS) at constant pressures of 40 mmHg (Fig. 1a**, time-lapse**). Histology of acellular kidneys showed preservation of tissue architecture and the complete removal of nuclei and cellular components (Fig. 1b**, time-lapse**). Perfusion decellularization preserved the structure and composition of renal ECM integral in filtration (glomerular basement membrane), secretion, and reabsorption (tubular basement membrane). As seen with other tissues, the arterial elastic fiber network remained preserved in acellular cortical and medullary parenchyma. Immunohiostochemical staining confirmed presence of key ECM components such as Laminin and Collagen IV in physiologic distribution such as the acellular glomerular basement membrane (Fig. 1c,d). The microarchitecture of the lobulated

Author Manuscript Author Manuscript Author Manuscript Author Manuscript

glomerular basement membrane with capillary and mesangial matrix extending from the centrilobular stalk remained intact. Acellular glomeruli were further encompassed by a multilayered corrugated and continuous Bowman's capsule basement membrane (Fig. 1e,f). Tubular basement membranes remained preserved with dentate evaginations extending into the proximal tubular lumen. SDS, deionized water, and Triton-X 100 reduced the total DNA content per kidney to less than 10% (Fig. 1g). After PBS washing, SDS was undetectable in acellular kidney scaffolds. Concentrations of ECM total collagen and glycosaminoglycans were preserved at levels not significantly different from cadaveric kidney tissue (Fig. 1h). To confirm scalability of the perfusion decellularization protocol to large animal and human kidneys, we successfully decellularized porcine and human kidneys using a similar perfusion protocol (Fig. 2a-d). Preservation of perfusable channels along a hierarchical vascular bed was confirmed by dye perfusion similar to our prior experience with perfusion decellularized hearts and lungs (Supplementary Fig. 1). Functional testing of acellular kidney scaffolds by perfusion of the vasculature with modified Krebs-Henseleit solution under physiologic perfusion pressure resulted in production of a filtrate high in protein, glucose and electrolytes suggesting hydrostatic filtration across glomerular and tubular basement membranes with loss of macromolecular sieving and active reabsorption.

To assess the microarchitecture of acellular kidney scaffolds, we applied an established histology-based morphometry protocol to quantify the average number of glomeruli, glomerular diameter, glomerular capillary lumen, and partial Bowman's space[20]. The total number of glomeruli remained unchanged between cadaveric and decellularized kidney cross sections through the hilum (12380.25±967.37 vs. 14790.35±2504.93, p=0.931). Glomerular diameter, Bowman's space and glomerular capillary surface area did not differ between cadaveric and decellularized kidneys (Supplementary Table 1).

Recellularization of acellular kidney scaffolds

To regenerate functional kidney tissue we repopulated acellular rat kidneys with endothelial and epithelial cells. We instilled suspended human umbilical venous endothelial cells (HUVEC) via the renal artery and suspended rat neonatal kidney cells (NKC) via the ureter. Cell delivery and retention improved when kidney scaffolds were mounted in a seeding chamber under vacuum to generate a pressure gradient across the scaffold (Fig. 3a). Attempts to seed NKCs applying positive pressure to the collecting system did not reach the glomerulus, while cell seeding using a transrenal gradient allowed for cell dispersion throughout the entire kidney parenchyma. Vacuum exceeding 70cmH_2O led to tissue damage in calyxes and parenchyma, while a vacuum of 40 cmH_2O did not cause macroscopic or microscopic tissue damage or leakage of cells, which is consistent with data on isolated tubular basement membrane mechanical properties[21]. After seeding, kidney constructs were transferred to a perfusion bioreactor designed to provide whole organ culture conditions (Fig. 3b,c). After three to five days of perfused organ culture, HUVECs lined vascular channels throughout the entire scaffold cross section, from segmental, interlobar, and arcuate arteries to glomerular and peritubular capillaries (Fig. 3d). Because a variety of epithelial cell phenotypes in different niches along the nephron contribute to urine production, we elected to reseed a combination of rat NKCs via the ureter in addition to HUVECs via the renal artery. Freshly isolated, enzymatic digests of rat neonatal kidneys

Author Manuscript Author Manuscript Author Manuscript Author Manuscript

produced single-cell suspensions of NKCs consisting of a heterogeneous mixture of all kidney cell types including mostly epithelial, but also endothelial, and interstitial lineages. When cultured on cell culture plastic after isolation, 8% of adherent cells expressed podocin indicating a glomerular epithelial phenotype, 69% expressed Na/K-ATPase indicating a proximal tubular phenotype, and 25% expressed E-Cadherin indicating a distal tubular phenotype (data not shown). After cell seeding, kidney constructs were mounted in a perfusion bioreactor and cultured in whole organ biomimetic culture. An initial period of static culture enabled cell attachment, after which perfusion was initiated to provide oxygenation, nutrient supply and a filtration stimulus. Neonatal rats are unable to excrete concentrated urine due to immaturity of the tubular apparatus[22]. To accelerate *in vitro* nephrogenesis and maturation of NKCs in acellular kidney matrices, we supplemented the culture media with *in vivo* maturation signals such as glucocorticoids and catecholamines. We cultured the reseeded kidneys under physiologic conditions for up to twelve days. On histologic evaluation after as early as four days in culture, we observed repopulation of the renal scaffold with epithelial and endothelial cells with preservation of glomerular, tubular, and vascular architecture. NKCs and HUVECs engrafted in their appropriate epithelial and vascular compartments (Fig. 3e). The spatial relationship of regenerated epithelium and endothelium resembled the microanatomy and polarity of the native nephron providing the anatomic basis for water and solute filtration, secretion, and reabsorption. Immunostaining revealed densely seeded glomeruli with endothelial cells and podocytes. Across the entire kidney, podocytes appeared to preferentially engraft in glomerular regions, although occasional non site-specific engraftment was observed (Fig. 3f,g). Epithelial cells on glomerular basement membranes stained positive for β-1 integrin suggesting site-specific cell adhesion to ECM domains (Fig. 3h). Engrafted epithelial cells were found to reestablish polarity and organize in tubular structures expressing Na/K-ATPase and aquaporin similar to native proximal tubular epithelium. Similarly, epithelial cells expressing e-cadherin formed structures resembling native distal tubular epithelium and collecting ducts (Fig. 3e,h). E-cadherin positive epithelial cells lined the renal pelvis similar to native transitional epithelium. Transmission and scanning electron microscopy of regenerated kidneys showed perfused glomerular capillaries with engrafted podocytes and formation of foot processes (Fig. 3i,j). Morphometric analysis of regenerated kidneys showed recellularization of more than half of glomerular matrices, resulting in an average number of cellular glomeruli per regenerated kidney of approximately 70% of that of cadaveric kidneys. Average glomerular diameter, Bowman's space and glomerular capillary lumen were smaller in regenerated kidneys compared to cadaveric kidneys (Supplementary Table 2).

In vitro function of acellular and regenerated kidneys

After cell seeding and whole organ culture, we tested the *in vitro* capacity of regenerated kidneys to filter a standardized perfusate, to clear metabolites, to reabsorb electrolytes and glucose, and to generate concentrated urine (Fig. 4a). Decellularized kidneys produced nearly twice as much filtrate as cadaveric controls, while regenerated kidneys produced the least amount of urine. All three groups maintained a steady urine output over the testing period (Fig. 4b). Based on the results of urinalysis we calculated creatinine clearance as an estimate for glomerular filtration rate, and fractional solute excretion as a measure of tubular absorptive and secretory function (Fig. 4d**,** Supplementary Table 3). Due to increased dilute

Author Manuscript Author Manuscript Author Manuscript Author Manuscript

urine production, calculated creatinine clearance was increased in decellularized kidneys when compared to cadaveric kidneys indicating increased glomerular (and likely additional tubular and ductal) filtration across acellular basement membranes. After repopulation with endothelial and epithelial cells, creatinine clearance of regenerated constructs reached approximately 10% of cadaveric kidneys, which indicates a decrease of glomerular filtration across a partially reconstituted and likely immature glomerular membrane (Fig. 4c). Vascular resistance was found to increase with decellularization, and decrease after re-endothelialization, but remained higher in regenerated constructs compared to cadaveric kidneys (Fig. 4d). This finding is in line with prior observations in cardiac and pulmonary re-endothelialization and may be related to relative immaturity of the vascular bed and micro-emboli from cell culture media. When *in vitro* renal arterial perfusion pressure was increased to 120 mmHg, urine production and creatinine clearance in regenerated kidneys reached up to 23% of cadaveric kidneys (Fig. 4b,c). Albumin retention was decreased from 89.9% in cadaveric kidneys to 23.3% in decellularized kidneys, which is a level consistent with the estimated contribution of the denuded glomerular basement membrane to macromolecular sieving. With recellularizaton, albumin retention was partially restored to 46.9% leading to improved albuminuria in regenerated kidneys. Glucose reabsorption decreased from 91.7% in cadaveric kidneys to 2.8% after decellularization, consistent with free filtration and the loss of tubular epithelium. Regenerated kidneys showed partially restored glucose reabsorption of 47.38%, suggesting engraftment of proximal tubular epithelial cells with functional membrane transporters resulting in decreased glucosuria. Higher perfusion pressure did not lead to increased Albumin or Glucose loss in regenerated kidneys. Selective electrolyte reabsorption was lost in decellularized kidneys. Slightly more creatinine than electrolytes were filtered, leading to an effective fractional electrolyte retention ranging from 5-10%. This difference may be attributed to the electrical charge of the retained ions and the basement membrane[23], while the range amongst ions may be related to subtle differences in diffusion dynamics across acellular vascular, glomerular and tubular basement membranes. In regenerated kidneys, electrolyte reabsorption was restored to approximately 50% of physiologic levels, which further indicates engraftment and function of proximal and distal tubular epithelial cells. Fractional urea excretion was increased in decellularized kidneys, and returned to a more physiologic range in regenerated kidneys, which suggests partial reconstitution of functional collecting duct epithelium with urea transporters. For detailed urinalysis and fractional excretion see Supplementary Table 3.

Orthotopic transplantation and in vivo function of regenerated kidneys

Because we observed urine production *in vitro*, we hypothesized that regenerated kidneys could function *in vivo* after orthotopic transplantation. We performed experimental left nephrectomies and transplanted regenerated left kidneys in orthotopic position. We anastomosed regenerated left kidneys to the recipient's renal artery and vein (Fig. 4e). Throughout the entire test period, regenerated kidney grafts appeared well perfused without any evidence of bleeding from vasculature, collecting system or parenchyma (Fig. 4e). The ureter remained cannulated to document *in vivo* production of clear urine without evidence of gross hematuria and to collect urine samples. Regenerated kidneys produced urine from shortly after unclamping of recipient vasculature until the planned termination of the

Author Manuscript Author Manuscript Author Manuscript Author Manuscript

experiment. Histological evaluation of explanted regenerated kidneys showed blood-perfused vasculature without evidence of parenchymal bleeding or microvascular thrombus formation (Fig 4f). Corresponding to *in vitro* studies, decellularized kidneys produced a filtrate which was high in glucose (249±62.9 vs. 29±8.5 mg dL^{-1} in native controls) and albumin (26.85±4.03 vs. 0.6±0.4 g dL^{-1} in controls), while low in urea (18±42.2 vs. 617.3±34.8 mg dL^{-1} in controls), and creatinine (0.5±0.3 vs. 24.6±5.8 mg dL^{-1} in controls). Regenerated kidneys produced less urine than native kidneys (1.2±0.1 vs. 3.2±0.9 μl min^{-1} in native controls, 4.9±1.4 μl min^{-1} in decellularized kidneys) with lower creatinine (1.3±0.2 mg dL^{-1}) and urea (28.3±8.5 mg dL^{-1}) than native controls, but showed improved glucosuria (160±20 mg dL^{-1}) and albuminuria (4.67±2.51 g L^{-1}) when compared to decellularized kidneys. Similar to the *in vitro* results, creatinine clearance in regenerated kidneys was lower than that of native kidneys (0.01±0.002 vs. 0.36±0.09 ml min^{-1} in controls) as was urea excretion (0.003±0.001 vs. 0.19±0.01 mg min^{-1} in controls). *O*rthotopic transplantation of regenerated kidneys showed immediate graft function during blood perfusion via the recipient's vasculature *in vivo* without signs of clot formation or bleeding. Results of urinalysis corresponded to the *in vitro* observation of relative immaturity of the constructs.

Discussion

A bioengineered kidney derived from patient-derived cells and regenerated 'on demand' for transplantation could provide an alternative treatment for patients suffering from renal failure. While many hurdles remain, we describe a novel approach for creation of such a graft, and report three milestones: the generation of three-dimensional acellular renal scaffolds via perfusion decellularization of cadaveric rat, porcine, and human kidneys; the repopulation of endothelial and epithelial compartments of such renal scaffolds leading to the formation of viable tissue; and excretory function of the resulting graft during perfusion through its vasculature *in vitro* and after orthotopic transplantation *in vivo*.

In line with prior studies, we confirmed that detergent decellularization of whole rat, porcine, and human kidneys removes cells and cellular debris without disruption of vascular, glomerular, and tubular ultrastructure[14,16-18]. As expected, decellularization led to a loss of cell mediated functions such as macromolecular sieving, and solute transport. Glomerular and tubular basement membranes are permeable to macromolecules, small solutes and water, because filtration and reabsorption occur across these barriers in the native kidney[21,24]. Because macromolecule retention, secretion and reabsorption of metabolites and electrolytes, and regulation of an acid base equilibrium depend on viable endothelium and epithelium, we proceeded to repopulate acellular scaffolds with endothelial and immature epithelial cells[25]. While cell seeding of tissues such as muscle, vasculature, or trachea can be accomplished by surface attachment or intraparenchymal injection, repopulation of a more complex organ such as the kidney poses numerous challenges[26,27]. Similar to our prior experiments with lungs, we took advantage of preexisting vascular and urinary compartments, and seeded endothelial cells via the vascular tree and epithelial cells via the collecting system[13]. Length and diameter of acellular nephrons posed a major challenge to cell seeding from the urinary side. Tubule elasticity and permeability increase with decellularization, while tubular diameters increase with pressure[21]. In the present study,

Author Manuscript Author Manuscript Author Manuscript Author Manuscript

a transrenal pressure gradient during initial cell seeding substantially increased cell delivery and retention. Glomerular ECM structures predominantly repopulated with podocytes, while tubular structures repopulated with tubular epithelial cells with reestablished polarity. Such site-selective engraftment of podocytes on glomerular basement membranes highlights the value of native ECM in tissue regeneration. Laminins and Collagen IV are the major ECM proteins of the glomerular basement membrane and are necessary for podocyte adhesion, slit diaphragm formation and glomerular barrier function[28,29]. Immunohistochemical staining of matrix cross-sections in our study showed preservation of these proteins within the glomerular basement membrane after perfusion decellularization. *In vitro*, α3β1 integrin mediates rat podocyte adhesion and regulates anchorage-dependent growth and cell cycle control[30,31]. Preserved glomerular basement membrane proteins in decellularized kidney scaffolds, and β1-integrin expression in engrafted podocytes suggest site-specific cell adhesion to physiologic ECM domains.

After several days in organ culture regenerated kidney constructs produced urine *in vitro*. The intact whole organ architecture of regenerated kidneys provided a unique opportunity for global functional testing, and assessment of *in vivo* function after transplantation. In regenerated kidneys, macromolecular sieving, glucose and electrolyte reabsorption were partially restored, indicating engraftment and function of endothelial cells, podocytes, and tubular epithelial cells. Glomerular filtration rate in regenerated kidneys was lower compared to cadaveric kidneys – in part a result of increased vascular resistance resulting in decreased graft perfusion. Creatinine clearance improved with increased renal arterial perfusion pressures. Fractional reabsorption of electrolytes did not reach the levels of cadaveric kidneys, which could be related to incomplete seeding and the immature stage of seeded neonatal epithelial cells[22]. Further maturation of the cell-seeded constructs will likely improve vascular patency and control of electrolyte reabsorption[28]. Despite this functional immaturity, regenerated kidney constructs provided urine production and clearance of metabolites after transplantation *in vivo*. We did not observe bleeding or graft thrombosis during perfusion via the recipient's vascular system. Successful orthotopic transplantation in rats demonstrates the advantage of physiologic graft size and anatomic features such as renal vascular conduits and ureter. Once developed further, bioengineered kidneys could become a fully implantable treatment option for renal support in end stage kidney disease.

In summary, cadaveric kidneys can be decellularized, repopulated with endothelial and epithelial cells, matured to functional kidney constructs *in vitro*, and transplanted in orthotopic position to provide excretory function *in vivo*. Translation of this technology beyond proof of principle will require optimization of cell seeding protocols to human-sized scaffolds, upscaling of biomimetic organ culture, as well as isolation, differentiation, and expansion of the required cell types from clinically feasible sources.

Methods

Perfusion decellularization of kidneys

We isolated a 68 rat kidneys for perfusion decellularization. All animal experiments were performed in accordance with the Animal Welfare Act and approved by the institutional animal care and use committee at the Massachusetts General Hospital. We anesthetized

Author Manuscript Author Manuscript Author Manuscript Author Manuscript

male, 12-week-old, Sprague-Dawley rats (Charles River Labs) using inhaled 5% isoflurane (Baxter). After systemic heparinization (American Pharmaceutical Partners) through the infrahepatic inferior vena cava, a median laparotomy exposed the retroperitoneum. After removal of Gerota's fascia, perirenal fat, and kidney capsule, we transected the renal artery, vein, and ureter and retrieved the kidney from the abdomen. We cannulated the ureter with a 25-gauge cannula (Harvard Apparatus). Then, we cannulated the renal artery with a prefilled 25-guage cannula (Harvard Apparatus) to allow antegrade arterial perfusion of heparinized PBS (Invitrogen) at 30mmHg arterial pressure for 15-minutes to rid the kidney of residual blood. We then administered decellularization solutions at 30mmHg constant pressure in order: 12-hours of 1% SDS (Fisher) in deionized water, 15-minutes of deionized water, and 30-minutes of 1% Triton-X-100 (Sigma) in deionized water. Following decellularization, we washed the kidney scaffolds with PBS containing 10,000 U/mL penicillin G, 10 mg/mL streptomycin, and 25 μg/mL amphotericin-B (Sigma) at 1.5 mL/min constant arterial perfusion for 96-hours.

Rat neonatal kidney cell isolation

We euthanized day 2.5-3.0 Sprague-Dawley neonates for organ harvests. We then excised both kidneys via median laparotomy and stored them on ice (4°C) in Renal Epithelial Growth Media (REGM, Lonza). We transferred kidneys to a 100mm culture dish (Corning, Corning, NY) for residual connective tissue removal and subsequent mincing into $<1mm^3$ pieces. The renal tissue slurry was resuspended in 1mg/mL Collagenase I (Invitrogen) and 1mg/mL Dispase (StemCell Technologies) in DMEM (Invitrogen), and incubated in a 37°C shaker for 30-minutes. The resulting digest slurry was strained (100μm; Fisher) and washed with 4°C REGM. We then resuspended non-strained tissue digested in collagenase/dispase as described above and repeated incubation, straining, and blocking. The resulting cell solution was centrifuged (200g, 5-minutes), and cell pellets were resuspended in 2.5mL REGM, counted, and seeded into acellular kidney scaffolds as described below.

Human umbilical vein endothelial cell subculture and preparation

We expanded m-cherry labeled human umbilical vein endothelial cells passages 8-10 on gelatin-a (BD Biosciences) coated cell culture plastic and grown with Endothelial Growth Medium-2 (EGM2, Lonza). At the time of seeding, cells were trypsinized, centrifuged, resuspended in 2.0mL of EGM2, counted, and subsequently seeded into decellularized kidneys as described below.

Cell seeding

We trypsinized and diluted $50.67\pm12.84\times10^6$ human umbilical vein endothelial cells (HUVEC) in 2.0 mL EGM-2 and seeded these onto the acellular kidney scaffold via the arterial cannula at 1.0 mL/min constant flow. Cells were allowed to attach overnight after which perfusion culture resumed. $60.71\pm11.67\times10^6$ rat neonatal kidney cells were isolated following the procedure described above, counted, and resuspended in 2.5 mL of REGM. The cell suspension was seeded through the ureter cannula after subjugating the organ chamber to a -40 cmH_2O pressure. Cells were allowed to attach overnight after which perfusion culture resumed.

Author Manuscript Author Manuscript Author Manuscript Author Manuscript

Bioreactor design and whole organ culture

We designed and custom built the kidney bioreactor as a closed system that could be gas sterilized after cleaning and assembly, needing only to be opened once at the time of organ placement. Perfusion media and cell suspensions were infused through sterile access ports (Cole-Parmer) to minimize the risk of contamination. Media was allowed to equilibrated with 5% CO_2 95% room air by flowing through a silicone tube oxygenator (Cole-Parmer) before reaching the cannulated renal artery 1.5mL/min. The ureter and vein were allowed to drain passively through into the reservoir during biomimetic culture.

Isolated kidney experiments

To assess *in vitro* kidney function, we perfused single native, regenerated, and decellularized kidneys with 0.22 μm-filtered (Fisher) Krebs-Henseleit (KH) solution containing: $NaHCO_3$ (25.0 mM), NaCl (118 mM), KCl (4.7 mM), $MgSO_4$ (1.2 mM), NaH_2PO_4 (1.2 mM), $CaCl_2$ (1.2 mM), BSA (5.0 g/dL), D-glucose (100 mg/dL), urea (12 mg/dL), creatinine (20 mg/dL), (Sigma Aldrich). We added amino acids glycine (750 mg/L), L-alanine (890 mg/L), L-asparagine (1,320 mg/L), L-aspartic acid (1330 mg/L), L-glutamic acid (1470 mg/L), L-proline (1150 mg/L), and L-serine (1050 mg/L) prior to testing (Invitrogen). KH solution was oxygenated (5% CO_2, 95% O_2), warmed (37° C), and perfused through the arterial cannula at 80-120 mmHg constant pressures without recirculation. Urine and venous effluent passively drained into separate collection tubes. We took samples at 10, 20, 30, 40, and 50-minutes after initiating perfusion, and froze them immediately −80° C until analyzed. Urine, venous effluent, and perfusing KH solutions were quantified using a Catalyst Dx Chemistry Analyzer (Idexx, Westbrook, ME). We calculated the vascular resistance (RVR) as arterial pressure (mmHg)/renal blood flow (ml/g/min). After completion of *in vitro* experiments, we flushed kidneys with sterile PBS, decannulated them, and transferred to a sterile container in cold (4°C) PBS until further processing.

A detailed description of methods used for histology, electron microscopy, scaffold analysis, and orthotopic transplantation are available online as supplemental material.

Supplementary Material

Refer to Web version on PubMed Central for supplementary material.

Acknowledgements

The present study was supported by the NIH Director's New Innovator Award DP2 OD008749-01, and departmental funds. JJS was supported by an AΩA Research Fellowship, and an AHA Predoctoral Fellowship. The PMB Microscopy Core is supported by NIH grants DK43351 and DK57521. We would further like to thank Qi C Ott for critical review and editing of the manuscript. We would like to thank Chris Hoffman, John Beagle, and Michael Duggan for technical support with urine sample analysis. We would like to thank Mary McKee for her expert support with transmission electron microscopy and Ann Tisdale for her expert support with scanning electron microscopy.

References

1. (CDC). C.f.D.C.a.P. National chronic kidney disease fact sheet: general information and national estimates on chronic kidney disease in the United States, 2010. U.S. Department of Health and Human Services (HHS), CDC; Atlanta, GA: 2010.

Author Manuscript Author Manuscript Author Manuscript Author Manuscript

2. OPTN: Organ Procurement and Transplantation Network Website. 2012
3. Kawai T, et al. HLA-mismatched renal transplantation without maintenance immunosuppression. N Engl J Med. 2008; 358:353–361. [PubMed: 18216355]
4. Humes HD, Krauss JC, Cieslinski DA, Funke AJ. Tubulogenesis from isolated single cells of adult mammalian kidney: clonal analysis with a recombinant retrovirus. The American journal of physiology. 1996; 271:F42–49. [PubMed: 8760242]
5. Humes HD, MacKay SM, Funke AJ, Buffington DA. Tissue engineering of a bioartificial renal tubule assist device: in vitro transport and metabolic characteristics. Kidney international. 1999; 55:2502–2514. [PubMed: 10354300]
6. Humes HD, Buffington DA, MacKay SM, Funke AJ, Weitzel WF. Replacement of renal function in uremic animals with a tissue-engineered kidney. Nat Biotechnol. 1999; 17:451–455. [PubMed: 10331803]
7. Humes HD, et al. Initial clinical results of the bioartificial kidney containing human cells in ICU patients with acute renal failure. Kidney international. 2004; 66:1578–1588. [PubMed: 15458454]
8. Humes HD, Weitzel WF, Fissell WH. Renal cell therapy in the treatment of patients with acute and chronic renal failure. Blood Purif. 2004; 22:60–72. [PubMed: 14732813]
9. Rogers SA, Hammerman MR. Prolongation of life in anephric rats following de novo renal organogenesis. Organogenesis. 2004; 1:22–25. [PubMed: 19521556]
10. Gura V, Macy AS, Beizai M, Ezon C, Golper TA. Technical breakthroughs in the wearable artificial kidney (WAK). Clin J Am Soc Nephrol. 2009; 4:1441–1448. [PubMed: 19696219]
11. Fissell WH, Roy S. The implantable artificial kidney. Semin Dial. 2009; 22:665–670. [PubMed: 20017839]
12. Ott HC, et al. Perfusion-decellularized matrix: using nature's platform to engineer a bioartificial heart. Nat Med. 2008; 14:213–221. [PubMed: 18193059]
13. Ott HC, et al. Regeneration and orthotopic transplantation of a bioartificial lung. Nat Med. 2010; 16:927–933. [PubMed: 20628374]
14. Nakayama KH, Batchelder CA, Lee CI, Tarantal AF. Decellularized rhesus monkey kidney as a three-dimensional scaffold for renal tissue engineering. Tissue Eng Part A. 2010; 16:2207–2216. [PubMed: 20156112]
15. Ross EA, et al. Embryonic Stem Cells Proliferate and Differentiate when Seeded into Kidney Scaffolds. Journal of the American Society of Nephrology. 2009; 20:2338–2347. [PubMed: 19729441]
16. Orlando G, et al. Production and Implantation of Renal Extracellular Matrix Scaffolds From Porcine Kidneys as a Platform for Renal Bioengineering Investigations. Annals of surgery Publish Ahead of Print. 2012 10.1097/SLA.1090b1013e31825a31802ab.
17. Song JJ, Ott HC. Organ engineering based on decellularized matrix scaffolds. Trends Mol Med. 2011; 17:424–432. [PubMed: 21514224]
18. Sullivan DC, et al. Decellularization methods of porcine kidneys for whole organ engineering using a high-throughput system. Biomaterials. 2012
19. Atala A, Bauer SB, Soker S, Yoo JJ, Retik AB. Tissue-engineered autologous bladders for patients needing cystoplasty. Lancet. 2006; 367:1241–1246. [PubMed: 16631879]
20. Olivetti G, Anversa P, Rigamonti W, Vitali-Mazza L, Loud AV. Morphometry of the renal corpuscle during normal postnatal growth and compensatory hypertrophy. A light microscope study. J Cell Biol. 1977; 75:573–585. [PubMed: 264124]
21. Welling LW, Grantham JJ. Physical properties of isolated perfused renal tubules and tubular basement membranes. J Clin Invest. 1972; 51:1063–1075. [PubMed: 5057126]
22. Falk G. Maturation of renal function in infant rats. Am J Physiol. 1955; 181:157–170. [PubMed: 14376587]
23. Bray J, Robinson GB. Influence of charge on filtration across renal basement membrane films in vitro. Kidney Int. 1984; 25:527–533. [PubMed: 6204098]
24. Deen WM, Lazzara MJ, Myers BD. Structural determinants of glomerular permeability. Am J Physiol Renal Physiol. 2001; 281:F579–596. [PubMed: 11553505]

Author Manuscript Author Manuscript Author Manuscript Author Manuscript

25. Humes HD. Acute renal failure: prevailing challenges and prospects for the future. Kidney Int Suppl. 1995; 50:S26–32. [PubMed: 8544431]
26. Quint C, et al. Decellularized tissue-engineered blood vessel as an arterial conduit. Proc Natl Acad Sci U S A. 2011; 108:9214–9219. [PubMed: 21571635]
27. Elliott MJ, et al. Stem-cell-based, tissue engineered tracheal replacement in a child: a 2-year follow-up study. Lancet. 2012; 380:994–1000. [PubMed: 22841419]
28. Dandapani SV, et al. Alpha-actinin-4 is required for normal podocyte adhesion. J Biol Chem. 2007; 282:467–477. [PubMed: 17082197]
29. Kretzler M. Regulation of adhesive interaction between podocytes and glomerular basement membrane. Microsc Res Tech. 2002; 57:247–253. [PubMed: 12012393]
30. Cybulsky AV, Carbonetto S, Huang Q, McTavish AJ, Cyr MD. Adhesion of rat glomerular epithelial cells to extracellular matrices: role of beta 1 integrins. Kidney Int. 1992; 42:1099–1106. [PubMed: 1280701]
31. Borza CM, et al. Human podocytes adhere to the KRGDS motif of the alpha3alpha4alpha5 collagen IV network. J Am Soc Nephrol. 2008; 19:677–684. [PubMed: 18235087]

Author Manuscript Author Manuscript Author Manuscript Author Manuscript

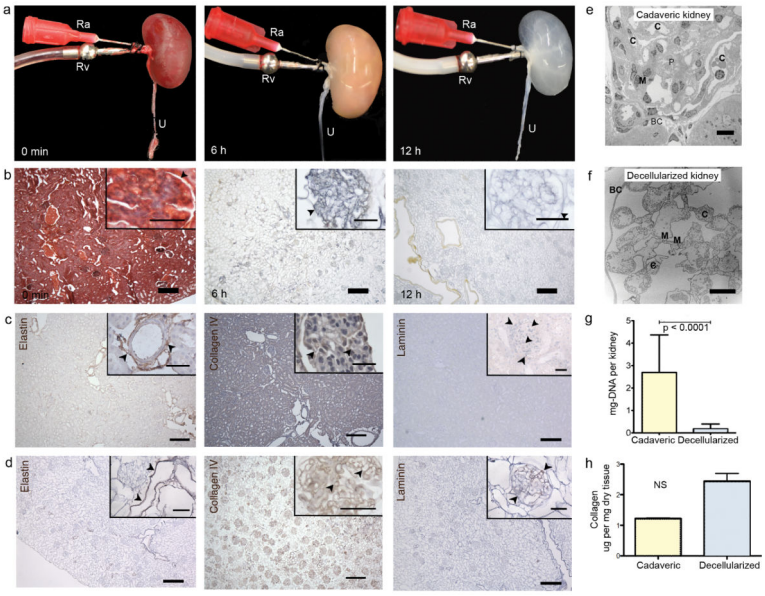

Figure 1. Perfusion decellularization of whole rat kidneys

(a) Time lapse photographs of a cadaveric rat kidney, undergoing antegrade renal arterial perfusion decellularization. *Ra*, renal artery; *Rv*, renal vein*; U*, ureter. A freshly isolated kidney (left); after 6 hours of SDS perfusion (middle); after 12 hours of SDS perfusion (right). **(b)** Representative corresponding Movat's Pentachrome stained sections of rat kidney during perfusion decellularization (black arrowheads showing Bowman's capsule, scale bar 250μm in main image, 50μm in insert). **(c)** Representative immunohistochemical stains of cadaveric rat kidney sections showing distribution of elastin (black arrowheads pointing at elastic fibers in tunica media of cortical vessels), collagen IV and laminin (black arrowheads highlighting glomerular basement membranes) (scale-bars 250μm in main image, 50μm in insert). **(d)** Corresponding sections of decellularized rat kidney tissue after immunohistochemical staining for elastin, collagen IV and laminin confirming preservation of extracellular matrix proteins in the absence of cells (scale-bars 250μm in main image, 50μm in insert). **(e)** Transmission electron micrograph (TEM) of a cadaveric rat glomerulus showing capillaries (C), mesangial matrix (M) and podocytes (P) surrounded by Bowman's capsule (BC) (scale bar 10μm). **(f)** TEM of decellularized rat glomerulus exhibiting acellularity in decellularized kidneys with preserved capillaries (C), mesangial matrix (M) and Bowman's space encapsulated by Bowman's capsule (BC) (scale bar 10μm). **(g,h)** Biochemical quantification of DNA and total collagen in cadaveric and decellularized rat kidney tissue (average ± SD, p-value determined by student's t-test) show reduction of DNA content and preservation of collagen after perfusion decellularization (NS: non significant).

Author Manuscript Author Manuscript Author Manuscript Author Manuscript

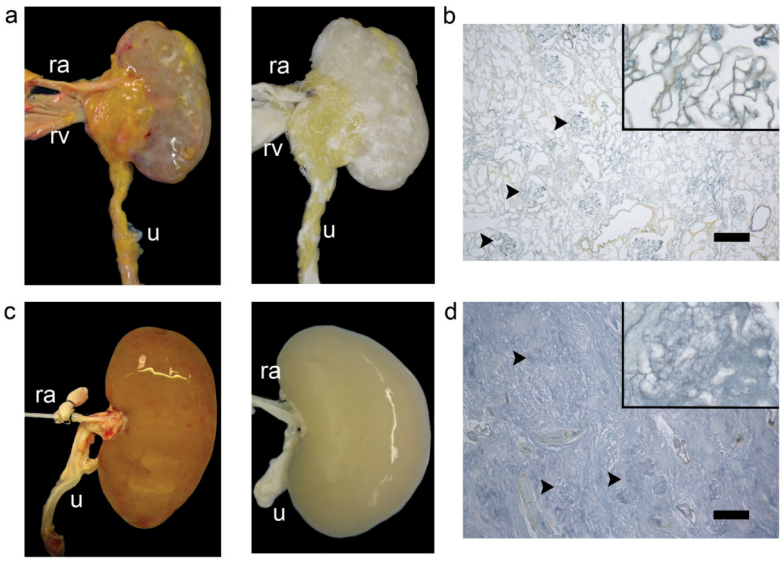

Figure 2. Perfusion decellularization of porcine and human kidneys

(a) Photograph of cadaveric (left) and decellularized (middle panels) porcine kidneys suggesting perfusion decellularization of rat kidneys may be upscaled to generate acellular kidney ECMs of clinically relevant size. Ra, renal artery; Rv, renal vein; Ur, Ureter. **(b)** Photograph of cadaveric (left) and decellularized (middle panels) human kidneys. **(c,d)** Corresponding Pentachrome staining for decellularized porcine and human kidneys (right panels, black arrowheads mark acellular glomeruli, scale bar 250um).

Author Manuscript Author Manuscript Author Manuscript Author Manuscript

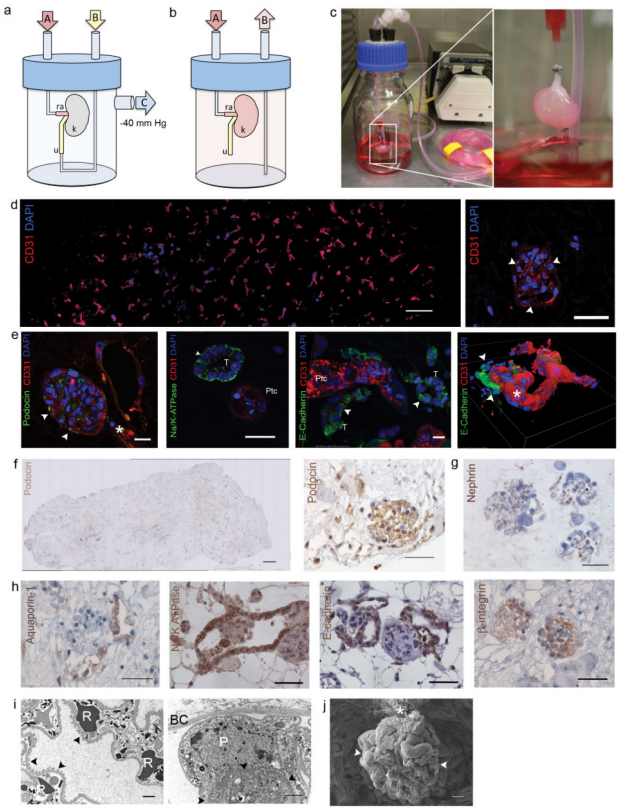

Figure 3. Cell seeding and whole organ culture of decellularized rat kidneys

(a) Schematic of a cell seeding apparatus enabling endothelial cell seeding via port A attached to the renal artery (ra), and epithelial cell seeding via port B attached to the ureter (u), while negative pressure in the organ chamber is applied to port C thereby generating a transrenal pressure gradient (left). **(b)** Schematic of a whole organ culture in a bioreactor enabling tissue perfusion via port A attached to the renal artery (ra) and drainage to a reservoir via port B (u, ureter; k, kidney). **(c)** Cell seeded decellularized rat kidney in whole organ culture. **(d)** Fluorescence micrographs of a re-endothelialized kidney constructs. CD31 (red) and DAPI-positive HUVECs line the vascular tree across the entire graft cross section (image reconstruction, left, scale bar 500 μm) and form a monolayer to glomerular capillaries (right panel, white arrowheads point to endothelial cells, scale bar 50μm). **(e)** Fluorescence micrographs of re-endothelialized and re-epithelialized kidney constructs showing engraftment of podocin (green) expressing cells and endothelial cells (CD31 positive, red) in a glomerulus (left panel, scale bar 25μm, white arrowheads mark Bowman's capsule, white star marks vascular pole); engraftment of Na/K ATPase expressing cells (green) in basolateral distribution in tubuli resembling proximal tubular structures with appropriate nuclear polarity (left middle panel, scale bar 10μm, T tubule, Ptc peritubular capillary); engraftment of E-cadherin expressing cells in tubuli resembling distal tubular structures (right middle panel, scale bar 10μm, T tubule, Ptc peritubular capillary); 3D reconstruction of a reendothlialzied vessel leading into a glomerulus (white arrowheads mark Bowman's capsule, white star marks vascular pole). **(f)** Image reconstruction of an entire graft cross section confirming engraftment of podocin expressing epithelial cells (left

Author Manuscript Author Manuscript Author Manuscript Author Manuscript

panel, scale bar 500μm). Representative immunohistochemical staining of a reseeded glomerulus showing podocin expression (right panel, scale bar 50μm). **(g)** Nephrin expression in regenerated glomeruli (left panel) and cadaveric control (right panel, scale bar 50μm). **(h)** Aquaporin-1 expression in regenerated proximal tubular structures (left panel, scale bar 50μm); Na/K ATPase expression in regenerated proximal tubular epithelium (middle left panel, scale bar 50μm); E-Cadherin expression in regenerated distal tubular epithelium (middle right panel, scale bar 50 μm); β-1 integrin expression in a regenerated glomerulus (right panel, scale bar 50 μm). **(i)** Representative transmission electron micrograph of a regenerated glomerulus showing a capillary with red blood cells (RBC), and foot processes along the glomerular basement membrane (black arrowheads)(left panel, scale bar 2μm), transmission electron micrograph of a podocyte (P) adherent to the glomerular basement membrane (black arrowheads)(right panel, scale bar 2μm, BC Bowman's Capsule). **(j)** Scanning electron micrograph of a glomerulus (white arrowheads) in a regenerated kidney graft cross section (vascular pedicle *, scale bar 10μm).

Author Manuscript Author Manuscript Author Manuscript Author Manuscript

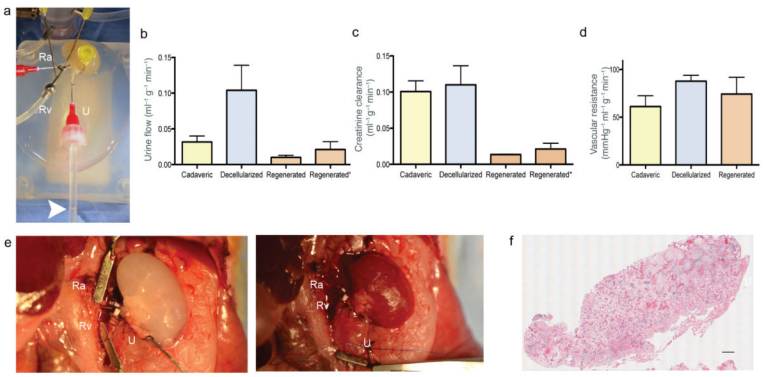

Figure 4. *In vitro* function of bioengineered kidney grafts and orthotopic transplantation

(a) Photograph of a bioengineered rat kidney construct undergoing *in vitro* testing. The kidney is perfused via the canulated renal artery (Ra), and renal vein (Rv), while urine is drained via the ureter (U). The white arrowhead marks the urine/air interface in the drainage tubing. **(b)** Bar graph summarizing average urine flow rate (mL/min) for decellularized, cadaveric, and regenerated kidneys perfused at 80mmHg and regenerated kidneys perfused at 120mmHg (regenerated*). Decelularized kidneys showed a polyuric state while regenerated constructs were relateively oliguric compared to cadaveric kidneys. **(c)** Bar graph showing average creatinine clearance in cadaveric, decellularized and regenerated kidneys perfused at 80mmHg and regenerated kidneys perfused at 120mmHg (regenerated*). With increased perfusion pressure creatinine clearance in regenerated kidneys improved. **(d)** Bar graph showing vascular resistance of cadaveric decellularized and regenerated kidneys showing an increase in vascular resistance with decellularization and partial recovery in regenerated kidneys. **(e)** Photograph of rat peritoneum after laparotomy, left nephrectomy, and orthotopic transplantation of a regenerated left kidney construct. Recipient left renal artery (Ra) and left renal vein (Rv) are connected to the regenerated kidney's renal artery and vein. The regenerated kidney's ureter (U) remained cannulated for collection of urine production post implantation (left panel); photograph of the transplanted regenerated kidney construct after unclamping of left renal artery (Ra) and renal vein (Rv) showing homogeneous perfusion of the graft without signs of bleeding. **(f)** Composite histologic image of a transplanted regenerated kidney confirming perfusion across the entire kidney cross section and the absence of parenchymal bleeding (scale bar 500 μm).